

Correspondence

Failure Detection and Isolation of Ultrasonic Ranging Sensors for Robotic Applications

Rogelio Luck and Asok Ray

Abstract—A failure detection and isolation (FDI) method for validation of ultrasonic ranging sensor (URS) signals in robot position control systems is presented. The technique builds upon the concepts of parity space and analytic redundancy where integration of analytic and sensor redundancy provides a direct, reliable method for measuring the end effector position of a robot relative to the world coordinates. These measurements are not influenced by deflections caused by the payload, accumulated joint measurement errors in a serial mechanism, and computational errors in executing kinematic relationships. The position control system's insensitivity to structural deflections allows the robot to handle larger payloads. Simulation results are presented to demonstrate how the FDI technique can be applied.

I. INTRODUCTION

One of the classical problems encountered in robotic systems design is the tradeoff between performance (e.g., accuracy and repeatability), load carrying capacity, and robot reach. Load carrying capacity could be measured as the robot's weight-to-payload ratio that is large for current robots [7] because robot position control systems are sensitive to deflections caused by the payload. Other factors, such as backlash, accumulated joint measurement errors in a serial mechanism, and computational errors in executing kinematic relationships, degrade the robot's performance and could hinder its capabilities for accurately moving objects to desired locations [8]–[11]. These difficulties could be partially circumvented by increasing the stiffness of the robot structure. However, an increase in stiffness is usually obtained at the expense of increased weight-to-payload ratio. Thus, to improve accuracy, the structure in many robotic designs are massive even for small payloads. A viable alternative, which addresses direct measurement of the end-effector position (or position error) to allow for a light robot structure, is presented in this paper.

In order to improve robustness of a robot position control system, the measurement of the end effector position should be as insensitive to noise and uncertainties as possible. The *a priori* knowledge about the structured uncertainties could be used to obtain enhanced estimations of the robot position [8]–[11]. If the robot is subjected to unstructured uncertainties, the indirect measurements based on the kinematic relationship may generate unacceptable errors in the end effector position. An alternative approach is to directly measure the position or position error of the robot end effector, and use of ultrasonic ranging sensors has been proposed to this effect [12]–[15].

Manuscript received January 30, 1988; revised September 30, 1988, and October 12, 1989.

R. Luck is with the Mechanical Engineering Department, Mississippi State University, Drawer ME, Mississippi State, MS 39762.

A. Ray is with the Mechanical Engineering Department, The Pennsylvania State University, University Park, PA 16802.

IEEE Log Number 8934167.

An ultrasonic ranging system (URS) that relies solely upon thresholding methods for detection of signals arriving at the receiver transducer (i.e., microphone for capturing audible signals) may yield a measurement uncertainty on the order of one wavelength of the signal [12], [16]. For example, assuming the velocity of sound in air to be 343 m/s, an accuracy of 0.025 mm would require the lower bound of frequency of transmission to be approximately 13.5 MHz. This is practically impossible to achieve since attenuation of acoustic signals varies directly with the square of the frequency resulting in noise corruption.

Significant improvement in accuracy of ultrasonic measurements that rely upon thresholding techniques can be achieved if the phase difference between transmitted and received ultrasonic waves is taken into account [17], [18]. Using this concept, Figueroa [12] has reported experimental results for position measurement with an uncertainty of ± 0.152 mm using a 40-kHz signal within a region of about 0.9 m radius and $\pm 25^\circ$ angular span. Figueroa has also suggested that, by careful control of the sources of errors in the ranging procedure, an accuracy of ± 0.025 mm can be attained.

A possible URS configuration consists of an ultrasonic transmitter located at the end effector of the robot and several ultrasonic receivers placed strategically in the vicinity of the workstation. To provide failure detection and isolation (FDI) capabilities [1]–[6] and ensure validity of the estimated position measurement, redundant receivers should be installed. The position measurements derived from the URS outputs are not prone to the errors that occur in the conventional position control systems [7], [19] due to the combined use of joint position measurements and robot kinematic models. The errors, resulting from uncertainties in the robot links and joints, position encoders and kinematic modeling, and mechanical vibrations could be eliminated at the cost of those due to URS noise and inaccuracy. Successful implementation of an URS for position control of a robotic end-effector largely depends upon the availability of an efficient algorithm to detect and isolate instrumentation failures and errors, and disturbances in acoustic wave propagation.

The objective of this paper is to develop a robust FDI methodology for validating measurements of the robot end-effector position by use of ultrasonic ranging sensors. This intelligent measurement system builds upon the concepts of *analytic redundancy* and *parity-space* that have been extensively used for signal validation in aerospace and nuclear instrumentation [1]–[6]. The following problems have been addressed in the paper.

- Criteria for placement of redundant ultrasonic receivers in the vicinity of a workstation.
- Detection and isolation of faulty or erroneous sensor data.
- Estimation of the end-effector position using the validated sensor data.

The paper is organized in seven sections and one appendix. Section II briefly describes the general configuration and salient operational features of the URS system under consideration. The measurement system model comprising both analytic and sensor redundancy is developed in Section III. The criteria for placement of redundant receivers are discussed in Section IV. A

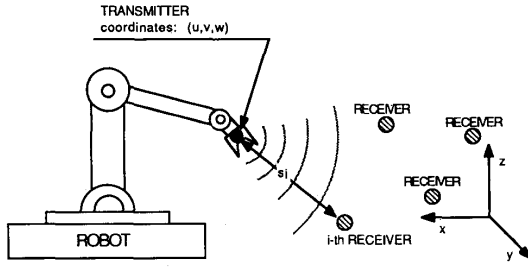


Fig. 1. Schematic of ultrasonic ranging system.

strategy for failure detection and isolation (FDI) is proposed in Section V. A simulation model of the URS system and pertinent results of simulation are presented in Section VI. The summary and conclusions of this paper are presented in Section VII. Appendix A outlines the underlying principles of the parity space concept.

II. GENERAL CONFIGURATION OF THE URS SYSTEM

A schematic diagram of the URS system under consideration is given in Fig. 1. This intelligent measurement system estimates the coordinates of the ultrasonic transmitter, located at the end-effector, with respect to a reference coordinate frame in the workstation area. The origin and the orientation of the reference frame are to be selected by the user. Given that the coordinates of the receiver transducers, i.e., ultrasonic "microphones," are known *a priori* with respect to the above reference frame, the transmitter measures its distance from each receiver. The quantity being measured is the amount of time an ultrasonic signal takes to travel from the transmitter to one of the receivers. This elapsed time is referred to as the *time of flight* or *acoustic distance* and is measured as the interval between the instants of signal transmission and reception of the microphone response. A counter is started when the ultrasonic signal is released, and the count ν is recorded when the signal arrives at the specified receiver and is detected by a thresholding technique. The time of flight τ_f is obtained from the recorded count ν after compensating for the signal phase angle and detection delay as

$$\tau_f = \left(\left(\nu + \frac{\phi}{2\pi} \right) / f \right) - E[\tau_d]$$

where f is the frequency (Hz) of the ultrasonic signal, ϕ is the phase difference (radians) between the transmitted and received signals, τ_d is the delay in detecting the signal at the receiver (τ_d may randomly vary with time and be different for individual receivers), and, $E[\bullet]$ denotes the expected value of \bullet .

Accurate measurements of ϕ are critical for evaluation of τ_f . Several phase detection techniques have been reported in literature. The techniques, proposed by Fox *et al.* [17] and Ono *et al.* [18], are based on frequency-modulated (FM) signals, offer relatively high accuracy in phase detection, and are essentially limited by the performance of electronic instrumentation. The basic principles of these two methods [17], [18] and a brief discussion on how they can be used for ultrasonic measurements in robotic applications are given in [12].

Next we proceed to evaluate the magnitude of the directed distance $\|s_i\|$ from the i th receiver to the transmitter as the product of the respective time of flight and average velocity of ultrasonic propagation in air. The measurements $\|s_i\|$, in addition to the electronic noise, are prone to uncertainties resulting from variations in atmospheric conditions such as temperature, humidity, turbulence, etc.

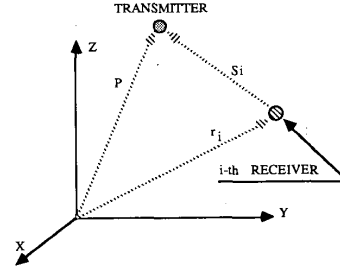


Fig. 2. Schematic of directed distances.

On the basis of this information from individual receivers, the instrumentation computer generates a validated estimate of the position vector of the end effector relative to the reference frame. The estimated value could be obtained either from single observations or from several observations using the concept of sequential testing [5], [20], [21].

III. DERIVATION OF THE SENSOR MODEL

The sensor model is derived in terms of the directed distances $\mathbf{p} = [u \ v \ w]^T$, \mathbf{r}_i , and s_i as shown in Fig. 2. The goal is to find \mathbf{p} given that both direction and magnitude of the directed distances $\mathbf{r}_i = [x_i \ y_i \ z_i]^T$, for the i th receiver, are completely known and only the magnitudes of the directed distances s_i are measurable for all $i = 1, 2, \dots, n$. Following Fig. 2, we have

$$s_i^T s_i = (\mathbf{p} - \mathbf{r}_i)^T (\mathbf{p} - \mathbf{r}_i), \quad i = 1, 2, \dots, n. \quad (1)$$

Defining $\delta_i = s_i^T s_i - \mathbf{r}_i^T \mathbf{r}_i$ yields

$$\delta_i = -2\mathbf{p}^T \mathbf{r}_i + \mathbf{p}^T \mathbf{p} \quad (2)$$

and rearranging (1) and (2), we obtain

$$\mathbf{d} = \mathbf{H}\mathbf{q} + \mathbf{e} \quad (3)$$

where

$$\mathbf{d} = \begin{bmatrix} \delta_1 \\ \delta_2 \\ \delta_3 \\ \vdots \\ \delta_n \end{bmatrix}, \quad \mathbf{H} = \begin{bmatrix} x_1 & y_1 & z_1 & 1 \\ x_2 & y_2 & z_2 & 1 \\ x_3 & y_3 & z_3 & 1 \\ \vdots & \vdots & \vdots & \vdots \\ x_n & y_n & z_n & 1 \end{bmatrix},$$

$$\mathbf{q} = [-2u \ -2v \ -2w \ \mathbf{p}^T \mathbf{p}]^T,$$

and $\mathbf{e} = [e_1 \ e_2, \dots, e_n]^T$ is the measurement error and noise vector.

The n -dimensional vector \mathbf{d} is the measurement vector, implying that the actual measurements, are modified using (2). The four-dimensional (4-D) vector \mathbf{q} may be interpreted to be a quaternion [22] or a directional distance with (u, v, w) as the vector part and $\mathbf{p}^T \mathbf{p}$ as the scalar instead of $(\mathbf{p}^T \mathbf{p})^{1/2}$ [23]. The $(n \times 4)$ measurement matrix \mathbf{H} is of rank 4 with the stipulation that any four rows are linearly independent. The rationale for this stipulation is discussed later. An advantage of using a sensor model of the form shown in (3) is that we may further express our confidence in each measurement by using a weighted least squares method to solve for \mathbf{q} . For instance, the optimal estimate of \mathbf{q} in the presence of measurement noise could be obtained from (3) as

$$\mathbf{q} = [\mathbf{H}^T \mathbf{K}^{-1} \mathbf{H}]^{-1} \mathbf{H}^T \mathbf{K}^{-1} \mathbf{d} \quad (4)$$

where \mathbf{K} is the measurement noise covariance matrix. The estimation procedure could be implemented by a linear tech-

nique (which is computationally simpler than the nonlinear estimation) for any $n \geq 4$. For $n > 4$, the least squares estimation [24] would be used. Furthermore, since $p^T p$ is nonlinearly related to u , v , and w , this approach generates an analytical redundancy [6] that verifies the consistency of the derived information. This is discussed in the next section.

The scale factor $p^T p$ provides an analytical redundancy which could be used to verify the consistency of the components u , v , and w via the nonlinear relation (2). We can specify a bound $\epsilon > 0$ such that $|u^2 + v^2 + w^2 - p^T p|^{1/2} \leq \epsilon$ must be satisfied for q to be an acceptable estimate. Otherwise, it implies that some or all of the measurements are erroneous.

IV. PLACEMENT OF RECEIVERS

The efficacy of the URS instrumentation for reliable control of end-effector positions is largely influenced by the placement of the receivers. Each row of the $(n \times 4)$ measurement matrix H in (5) corresponds to one individual receiver. Therefore, the position of each receiver with respect to others affects the relative dependence of the rows of H . It is desirable to have any four out of the n rows of H as nearly orthogonal to each other as possible in order to maximize the information contribution of the individual receivers. Ideally, no set of four receivers should be placed in such a way that it brings more information than any other set of four receivers. The advantage of this arrangement is that, in case of one failure in a set of redundant receivers, the remaining functioning units would provide enough information to obtain the location of the ultrasonic emitter albeit with less overall accuracy. An interesting characteristic of the sensor model is that the relative importance of the information obtained by each receiver is more strongly dependent on the location of the receivers relative to each other than on the location of the receivers relative to the transmitter (placed at the end effector).

From the structure of the matrix H , a relationship between the relative location of the receivers and row independence in H may not be immediately obvious. This is because of the fact that the receiver positions are defined in \mathcal{R}^3 but the rows of H are elements in \mathcal{R}^4 . The effects of the relative position of the receivers could be realized by augmenting the dimension of the position vector of each receiver from 3 to 4. A procedure for placing the receivers such that any four rows of H are assured to be linearly independent is presented as follows.

A mapping from \mathcal{R}^3 into \mathcal{R}^4 is defined as

$$f: \mathcal{R}^3 \rightarrow \mathcal{R}^4 \text{ such that } f(r) = [r^T \ 1]^T. \quad (5)$$

Then we generate a set Ω of position vectors in \mathcal{R}^4 from three different position vectors r_1 , r_2 and r_3 in \mathcal{R}^3 .

$$\Omega(r_1, r_2, r_3)$$

$$= \{\omega | \omega = \alpha f(r_1) + \beta f(r_2) + \gamma f(r_3); \alpha, \beta, \gamma \in \mathcal{R}\}. \quad (6)$$

It is important to note that $f(r_1)$, $f(r_2)$, and $f(r_3)$ are linearly dependent if there exists a number $\vartheta \in \mathcal{R}$ such that $r_1 = \vartheta r_2 + (1 - \vartheta)r_3$, which implies that the three receivers are colinear.

Given three noncolinear receivers with positions at r_1, r_2, r_3 , the problem is to define the relative location of the fourth position vector $\theta \in \mathcal{R}^3$ such that $f(r_1)$, $f(r_2)$, $f(r_3)$, and $f(\theta)$ are linearly independent in \mathcal{R}^4 .

To this effect we explicitly specify a set Θ in \mathcal{R}^3 such that

$$\Theta(r_1, r_2, r_3) = \{\theta | \theta \in \mathcal{R}^3; f(\theta) \in \Omega(r_1, r_2, r_3)\}. \quad (7)$$

Equation (7) is satisfied only if

$$f(\theta) = \alpha f(r_1) + \beta f(r_2) + \gamma f(r_3), \quad \alpha, \beta, \gamma \in \mathcal{R}. \quad (8)$$

Using (5) in (8), we obtain

$$[\theta^T \ 1]^T = [(\alpha r_1 + \beta r_2 + \gamma r_3)^T \ \alpha + \beta + \gamma]^T. \quad (9)$$

A comparison of individual elements in (9) yields

$$\alpha + \beta + \gamma = 1, \text{ and } \alpha r_1 + \beta r_2 + \gamma r_3 = \theta. \quad (10)$$

The significance of (10) is that the position vector θ lies in a plane passing through the tips of the three position vectors r_1 , r_2 , and r_3 . Thus, the set Θ of all $\theta \in \mathcal{R}^3$ that satisfies (10) is mapped under f into the set Ω of all four-dimensional vectors that are linearly dependent on $f(r_1)$, $f(r_2)$, and $f(r_3)$. We refer to this set Θ as the singularity plane on which three (noncolinear) receivers are located at r_1 , r_2 , and r_3 . Any redundant receiver lying on this singularity plane will result in four linearly dependent rows of H .

The implications of the previous analysis for placement of redundant receivers are summarized in the following.

No three receivers should be colinear; the best configuration would be an equilateral triangle. Once we have three receivers positioned, the fourth receiver should not be placed in the plane of the existing receivers. The best location for four receivers are the four corners of a tetrahedron. However, this ideal configuration may not always be possible to implement. By the same token, the fifth receiver should avoid the four distinct planes that are generated by the four triplet combinations of the existing receivers. Similarly, the $(n+1)$ st receiver should not be placed on any one of the $n!/(3!(n-3)!)$ planes.

V. FAILURE DETECTION AND MEASUREMENT ESTIMATION

Given that redundant receivers are available, the problem is how to detect and isolate receiver failures and to obtain a validated estimate of the end effector position. We define a fault as the transmittance of erroneous information to the instrumentation computer. Faults of large magnitudes resulting from abrupt disruptions, such as hardware failures and blocking of receivers are relatively easy to detect and isolate. It is the soft faults, i.e., gradual degradations over a long period of time such as those resulting from drifts in electronic amplifiers, which are difficult to diagnose. There are several approaches for dealing with soft faults [2], [3], [5]. In this paper we are proposing a methodology for sensor redundancy management, failure detection and isolation, and measurement estimation using the concepts of parity space and analytic redundancy that have been used for signal validation in aerospace and nuclear instrumentation [1]–[6]. A major difference between the URS model and conventional sensor models is that the unknown to be estimated is three dimensional but a mapping into a four dimensional space is necessary to obtain a linear redundancy. The concept of parity space is briefly described in Appendix A, and the details are reported by Potter and Suman [1]. A sensor redundancy management procedure using the parity space technique has been developed following the methodology of Ray and Desai [2] and is not presented in detail in this paper. A discussion on how to apply the concepts of parity space and analytic redundancy for fault diagnostics in URS systems follows.

The total number of measurements n needed to isolate r failures for an m -dimensional variable is given as $n \geq (2r + m)$ [1], [2]. We will refer to the number $\eta = (n - m)$ as the degree of linear redundancy. For example, when measuring a three dimensional variable, such as velocity or acceleration in inertial navigational units, five measurements are enough to detect and isolate a single failure, as $\eta = 2$ is needed to detect and isolate a single failure. Since $n = 4$ in the case of URS, six measurements ($\eta = 2$) are needed for isolation of any single failures, and five measurements ($\eta = 1$) can detect a failure but are not sufficient for its isolation by using the parity space technique.

Nevertheless, we have a (nonlinear) analytical redundancy, $p^T p = u^2 + v^2 + w^2$, which can be used in conjunction with one

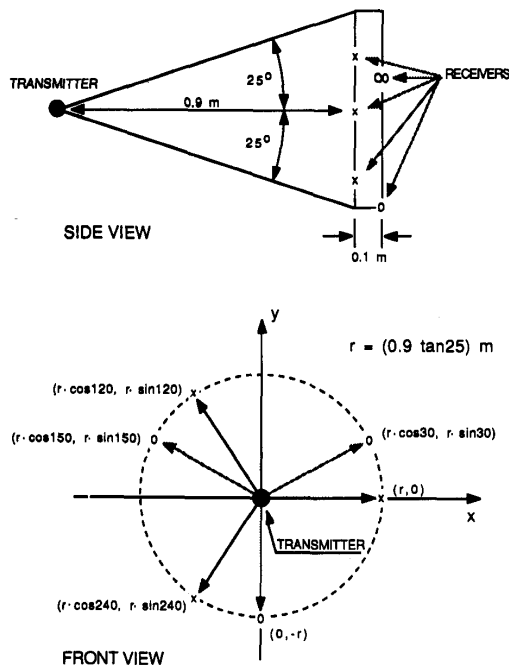


Fig. 3. Distribution of sensors.

degree of linear redundancy to isolate a single failure. With only four sensors, i.e., $\eta = 0$, single failures can be detected by using the analytical redundancy. This is discussed in Section VI.

The analytical redundancy due to $p^T p$ is used to verify the validity of the estimate after the parity space check. If $\eta > 1$, the estimate of the unknown q in (2) is obtained by a least squares method after isolating any fault(s). Validity of this estimate can be further checked using the analytic redundancy.

VI. SIMULATION RESULTS

Initial testing of the failure detection and isolation (FDI) technique was performed by simulation using a set of ultrasonic ranging sensors that are representative of those in a laboratory research facility. The model consists of six sensors symmetrically placed on the circumference of the bases of two cones with a common axis and vertex. The axis is parallel to the floor, and the emitter is located at the vertex with its coordinates as $(0, 0, 0)$. Three of the six receivers are positioned at 0° , 120° , and 240° on the circumference of the base of the first cone whose height is 0.9 meter and vertex angle is 50° . The remaining three receivers are positioned on the circumference of the base of the other cone that is 1.0 m high and the same base radius as the first cone. The sensor positions in the second cone are shifted by 30° relative to those in the first cone, their locations are at 30° , 150° , and 270° around the circumference of the second cone. Fig. 3 shows the above arrangement of sensors.

The reason for choosing the above configuration for the sensor assembly is that the two-dimensional parity space, generated from the six-dimensional (6-D) measurement space, has six parity axes of about the same magnitude and are equally distributed at intervals of 30° . The measurement matrix H in this sensor model produces a least square estimation matrix $[H^T H]^{-1} H^T$ whose columns have approximately the same

norm. This means that errors in each measurement have an almost identical bearing on the estimate of the measured variable.

Distances and orientations of individual sensors in the model were selected so as to satisfy the limitations of the actual hardware in a laboratory facility [12] with respect to ultrasonic microphones and the emitter. In this perspective the robot end effector, i.e., the emitter, was placed at the common vertex of the cones and the ultrasonic microphones positioned around the bases of these cones. The measurement matrix H resulting from this sensor configuration is given in the following:

$$H = \begin{bmatrix} 0.4226 & 0.9063 & 0.0000 & 1.0000 \\ 0.3660 & 0.9969 & 0.2113 & 1.0000 \\ -0.2113 & 0.9063 & 0.3660 & 1.0000 \\ -0.3660 & 0.9969 & 0.2113 & 1.0000 \\ -0.2113 & 0.9063 & -0.3660 & 1.0000 \\ 0.0000 & 0.9969 & -0.4226 & 1.0000 \end{bmatrix}$$

The sensor model is given by $d = Hq + e$. The emitter is located at the origin, i.e., the true value of the end effector position vector $x = [0 \ 0 \ 0]^T$ in \mathcal{R}^4 . Therefore, the measurements turn out to be the same as the sensor errors.

As mentioned earlier in Section V, the FDI technique builds upon the concept of the redundancy management procedure proposed by Ray and Desai [2]. This requires six quintuplets to be formed from the set of six sensors. Each quintuplet is labeled by the sensor it excludes. For each quintuplet, we select a submatrix containing five rows of the matrix H corresponding to the five sensors in the quintuplet. For instance, related to the quintuplet # i , the submatrix H_i excludes the i th row from the measurement matrix H . The parity vector related to each quintuplet is one-dimensional and the associated computational procedure is presented in detail in [3]. Following this procedure the FDI problem is reduced to checking the magnitudes of six one-dimensional (1-D) parity vectors followed by decisions on failures, if any. Appropriate thresholds are selected to check validity of each scalar parity entity under normal, unfailed conditions. Then a single failure could be detected and isolated since all scalar parity entities will have a large magnitude except for the parity entity related to the quintuplet that excludes the failed sensor. In this procedure, the effect of each and individual sensor error is included in the respective threshold.

As the degree of redundancy increases, checking of the parity entities in the FDI procedure becomes computationally burdensome because the number of quintuplets increases approximately on the order of the square of the number of sensors. In case of three or higher degrees of redundancy it may be more efficient to use the parity vector related to the original measurement matrix H itself. An alternative procedure, suggested by Ray, Desai and Deyst [4], is to specify a region in parity space which must enclose the parity vector under normal, unfailed operations. If the parity vector is not contained within this region, then the detection of a failure is implied and the faulty sensor may be isolated depending on the orientation of the parity vector. Simple examples of the above methodology are shown by Potter and Suman [1], Ray *et al.* [2], [4].

An outline for implementing the FDI algorithm, using a set of six or less sensors, is presented in the following.

Six Sensors: Six quintuplets are formed from the set of six sensor measurements. For each quintuplet the magnitude of the 1-D parity vector is computed, and a threshold is selected *a priori* on the basis of specified error bounds of individual sensors that belong to the quintuplet (see [2, (10)]). The failure decisions and measurement estimation are made as follows.

If all parity entities are larger than their respective thresholds, the failure cannot be isolated and none of the measurements are acceptable.

If all parity entities are smaller than their respective threshold, no failure is detected and a least square estimate of the emitter position is obtained using all six sensor data. The validity of the estimate is then checked by use of the nonlinear analytical redundancy test by comparing the quantity $|u^2 + v^2 + w^2 - p^T p|^{1/2}$ with an *a priori* specified threshold. At this stage the failure of the analytic redundancy test implies that the error vector lies in the column space of H ; the measurement set and the resulting estimate are unacceptable.

If exactly one parity entity (e.g., p_i formed from the i th quintuplet not containing the measurement $\#i$) is smaller than its threshold level, then the measurement $\#i$ is isolated as failed. The least squares estimate is obtained from the i th quintuplet. Validity of the estimate is checked by use of the nonlinear analytic redundancy as discussed above. This process is identical to that for a set of five unfailed sensors.

If some, but not all, of the six parity entities are smaller than their threshold levels, then the estimates are computed for each of the quintuplets whose parity entities are less than their respective thresholds. For each estimate, the analytical redundancy test is performed and only one quintuplet should pass this test. Otherwise, it should be concluded that the threshold settings are inconsistent or the failure lies in the column space of H .

Five Sensors: If only five measurements are available (i.e., if the degree of linear redundancy is one), the parity space approach is capable of failure detection only. With no failure, the procedure is similar to testing of the unfailed quintuplet as described previously. If a failure is detected, five quadruplets are formed out of the five measurements. For each quadruplet, validity of q , obtained as $H^{-1}d$ (note: H is a 4×4 invertible matrix), is checked by the analytical redundancy test for failure isolation. If a single failure has occurred, the quadruplet, not containing the failed measurement, should pass the test. Multiple failures cannot be isolated.

Four Sensors: If only four measurements are available (i.e., if the degree of linear redundancy is zero), the parity space approach is not applicable even for failure detection. The estimate is obtained as $q = H^{-1}m$. The analytic redundancy can check validity of q and thus serves as a recourse to failure detection.

Following the aforementioned FDI procedure, different types of faults were injected into the sensor assembly model. Simulation results agreed with the analytical derivations and were in line with experimental observations at the MIT nuclear research reactor for testing a similar FDI procedure [2]. Although these results were generated using a single sample approach, the FDI technique can be routinely extended to a sequential testing procedure as described in [5].

We examine the possible sources of error in the ultrasonic measurements before presenting the simulation results. Shoenwald *et al.* [25] discussed about noise interference in factory environment and possible ways to circumvent these problems. Bass and Bolen [26] obtained experimental results on ultrasonic background noise in industrial environments. Sources of noise such as metal parts being dropped into a bin, high speed grinding, bending of tubing, metal stamping, paint spraying, and laser etching were considered. With the exception of aerodynamic noise and laser etching, most sources were found to emit noise below 100 kHz. Their effects on the individual transducers are more or less similar and are therefore a source of common mode errors which can only be detected by use of the analytic redundancy. Since aerodynamic noise is well understood, devices can be constructed to mitigate the effects of these common mode disturbances. If the noise frequency exceeds 150 kHz, signal attenuation would occur within a short distance [12]

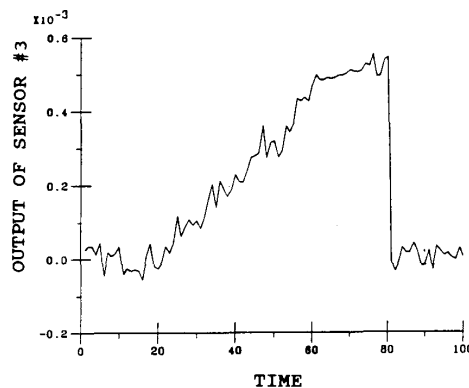


Fig. 4. Drift error in sensor output.

and therefore the noise may have non-identical effects on the individual transducers.

Sources of random errors associated with individual receivers include digitization of analog signals, vibration of the fixtures supporting the ultrasonic transducers, temperature fluctuations causing circuit parameter variations, aging of electronic equipment (e.g., drift in the clock frequency). Sources of errors that are common to all receivers include acoustic disturbances produced by other devices in the working environment and, to some extent, air turbulence. These errors when combined together may not be negligible. The cumulative effect can be approximated to be a sequence of white Gaussian noise at the individual receivers.

In the simulation we considered the noise in individual receivers to be predominant under normal operating conditions. Therefore the noise vector e in (3) was set to be zero mean, white Gaussian with standard deviation of 0.025 mm with independent and identical distribution for each sensor.

Large bias errors result when obstacles are placed in the path between receivers and transmitter or when a transducer fails abruptly. An obstruction either completely blocks the signal from reaching the receiver(s) or causes delays in the arrival of the signal since the signal travels longer distances after bouncing against several surfaces. On the other hand small bias errors may arise from malfunctions of electronic and mechanical components in the individual receivers.

Drifts in reference voltages, frequency counters, amplifier circuits etc., are expected to occur [12]. Also, the transducer response may drift with time at the operating frequency for reasons such as variations in temperature, humidity, etc. If an obstacle slowly approaches a receiver, the respective measurement may drift. Non-localized sources of error, i.e., common to all receivers, such as changes in pressure may result in errors. In such cases all measurements will be affected. If the error vector is contained in the column space of H , it will not be detected in the parity space but will exhibit inconsistency with respect to the (nonlinear) analytical redundancy, $p^T p = u^2 + v^2 + w^2$.

A fault in the form of a drift was injected in one of the sensors. This is shown in Fig. 4 as the mean of the sensor #3 data uniformly increasing from time 20 to 80. Fig. 5 exhibits comparison of the responses of the parity entities p_1 and p_3 generated from the quintuplets #1 and #3, respectively. All but the #3 quintuplet contains the faulty measurement #3. Therefore, the parity entity p_3 associated with the quintuplet #3 is not affected by the drift in sensor #3 whereas the parity entity associated with the other quintuplets (only p_1 is shown in Fig. 5) drift along with the sensor #3 data. The threshold level for each

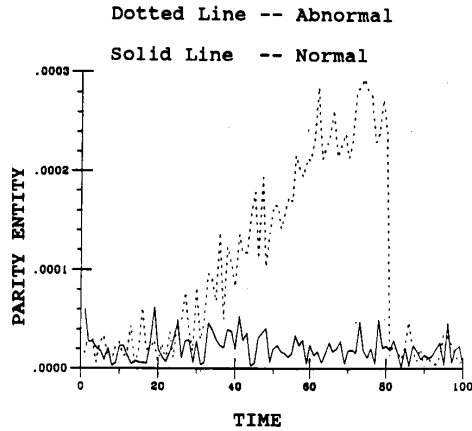


Fig. 5. Comparison of normal and abnormal parity entities.

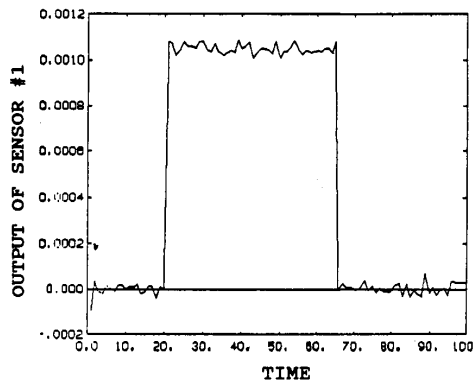


Fig. 6. Sample of undetected error in parity space.

parity entity was set slightly below 0.0001, which is approximately 1.5 times the average noise peaks under normal conditions. The FDI algorithm successfully isolated the sensor #3 as failed. No failure was detected in the time interval between 0 and 32 in Fig. 5. The failure (on a single sample basis) was detected and isolated at time 33 for the first time. A sequential test procedure would have indicated a failure at a later time close to 50. As the drift was eliminated after time 80, the test indicated normal functioning. This implies that the FDI technique functions normally after the source of error has been removed.

A constant bias error was added to the measurement vector d between the time interval 20 to 65 to illustrate how the nonlinear analytical redundancy is used in the FDI technique. The bias error vector was generated by a linear combination of all four columns of H with an identical weight of 0.45×10^{-3} for each column. Error vectors lying in the column space of H are not detectable by the parity space approach as they are projected onto the origin in the parity space. This implies that all six measurements are contaminated with the bias error. Fig. 6 shows the profile of the sensor #1 indicating the presence of a bias error. As expected, none of the parity entities were affected by the bias and thus the fault was undetected. The estimate q was generated from all six sensor data and its validity was tested by the analytic redundancy. Since the analytical redundancy is nonlinear, it is able to detect the fault by comparing the analytic

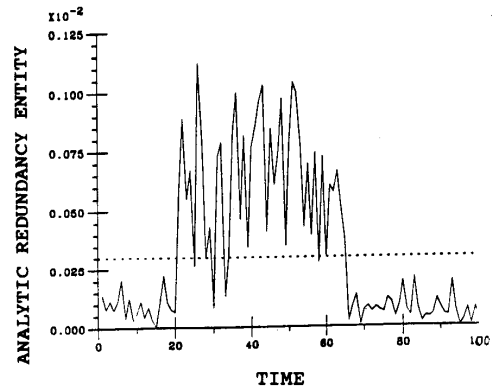


Fig. 7. Analytical redundancy.

redundancy entity, $|u^2 + v^2 + w^2 - p^T p|^{1/2}$ with the *a priori* selected threshold of 0.3×10^{-3} . The test detected the failure and invalidity of the estimate q during the time interval 20 to 65. The response of analytic redundancy entity for this bias error is shown in Fig. 7.

VII. CONCLUSION

A direct, reliable method has been proposed for measuring the end effector position of a robot by use of ultrasonic ranging sensors (URS). The intelligent measurement system consists of an ultrasonic transmitter (which is located at the end effector) and an array of redundant receivers. The positions of the receivers are known *a priori* relative to the reference frame, and the transmitter directly measures the distance from each of the receivers. On the basis of this information, the instrumentation computer detects and isolates sensor failures, and generates a validated estimate of the end effector position vector relative to the reference frame.

The previous method can be possibly extended to measurements of six-dimensional position and orientation vectors. This would require installation of at least two transmitters at the end effector. These transmitters will independently generate validated measurements of 3-D position vectors. Determination of relative locations of the transmitters and the associated bound on accuracy of the orientation measurement are a subject of future research.

The failure detection and isolation (FDI) procedure builds upon the concepts of *parity space* and *analytic redundancy* that have been extensively used for aerospace and nuclear instrumentation; these concepts have not apparently been applied so far in robotic instrumentation. The parity space technique allows for failure detection and isolation as well as a (weighted) least-square estimation of the end effector position from the linearly redundant sensor data. The analytic redundancy provides an additional nonlinear relationship which could be used for fault isolation and validation of the estimated end effector position. The key features of the proposed method are summarized below.

A minimum of four receivers are needed for the end effector position measurement and detection of a single failure. These four sensors must not be coplanar, and should be ideally placed on the four corners of a tetrahedron.

At least five receivers are required for isolation of single failures and a validated estimate of the end-effector position vector.

The measurement of the end effector position is independent of the errors due to structural deflections, joint inaccuracies, and kinematic computations. This direct measurement procedure would increase the robot's load carrying capacity in the sense that the position control system would not be sensitive to the structural deflections due to a varying payload.

The proposed measurement procedure is not restricted to robotic systems. It is applicable to any processes that use ultrasonic or laser ranging sensors for 3-D position measurements.

APPENDIX A

The Concept of Parity Space

A simplified model that includes only the zero-mean additive noise e is presented below. (Ray and Desai [3] have shown how to compensate for bias and scale factor errors in the sensor model.)

$$d = Hq + e. \quad (11)$$

Failure decisions should be made by concurrent checking of consistency and inconsistency of individual measurements at each time sample. (Precise definitions of the above terms in italics and their physical significance are given in [2].) A measure of relative consistencies between redundant measurements is given by the projection of the measurement vector d onto the left null space of the measurement matrix H such that the variations in the underlying variable Hq in (11) are eliminated and only the effects of the noise vector are observed. An $((n-4) \times n)$ matrix V is chosen such that its $(n-4)$ rows form an orthonormal basis for the left null space of H , i.e.,

$$VH = 0 \quad \text{and} \quad VV^T = I_{n-4}. \quad (12)$$

The column space of V is known as the parity space of H and the projection of d onto the parity space as the parity vector [1] that is given as

$$r = Vd = Ve. \quad (13)$$

From (12), it follows that

$$V^T V = I_n - H[H^T H]^{-1} H^T. \quad (14)$$

Because of the idempotent property of $V^T V$, the norm of the projection $V^T V d$ of d onto the left null space of H is identically equal to the form of r . The columns, v_1, v_2, \dots, v_{n-4} of V that are projections of the measurement directions (in \mathcal{R}^n) onto the parity space are called failure directions since the failure of the i th measurement m implies the growth of the parity vector r in (13) in the direction of v_i . For nominally unfailed operations, $r^T r$ remains small. If a failure occurs, r may (in time) grow in magnitude along the failure subspace, i.e., the subspace spanned by the specific column vectors associated with the failed measurements; and if the fault is time-dependent, then the failure directions (and hence the failure subspace) may also be time-dependent. The increase in the magnitude of the parity vector signifies abnormality of one or more measurements and its direction can be used for identification of abnormal measurement(s).

ACKNOWLEDGMENT

The authors acknowledge the benefits of discussion with Dr. Jorge Fernando Figueroa.

REFERENCES

- [1] J. E. Potter and M. C. Suman, "Thresholdless redundancy management with arrays of skewed instruments," *Integrity in Electronic Flight Control Systems*, vol. AGRADOGRAPH-224, pp. 15-1-15-25, 1977.
- [2] A. Ray and M. Desai, "A redundancy management procedure for fault detection and isolation," *ASME J. Dynamic Syst. Measurement Contr.*, pp. 248-254, Sept. 1986.
- [3] A. Ray and M. Desai, "A calibration and estimation filter for multiply redundant measurement systems," *ASME J. Dynamic Syst. Measurement Contr.*, pp. 149-156, June 1984.
- [4] A. Ray, M. Desai, and J. Deyst, "Fault detection and isolation in a nuclear reactor," *J. Energy*, vol. 7, no. 1, pp. 79-85, Jan.-Feb. 1983.
- [5] A. Ray, "Sequential testing for fault detection in multiply-redundant measurement systems," *ASME J. Dynamic Syst. Measurement Contr.*, pp. 329-332, June 1989.
- [6] E. C. Chow and A. S. Willsky, "Analytical redundancy and the design of robust failure detection systems," *IEEE Trans. Automatic Contr.*, vol. AC-29, pp. 603-614, July 1984.
- [7] J. Y. S. Luh, "Conventional controller design for industrial robots—A tutorial," *IEEE Trans. Syst. Man Cybern.*, vol. SMC-13, no. 3, pp. 298-316, 1983.
- [8] N. G. Dagalakis and D. K. Myers, "Adjustment of robot joint backlash using the robot joint test excitation technique," *The Int. J. Robotics*, vol. 4, no. 2, pp. 65-79, 1985.
- [9] F. Azadivar, "The effects of joint position errors of industrial robots on their performance in manufacturing operations," *IEEE J. Robotics Automat.*, vol. RA-3, no. 2, pp. 109-114, Apr. 1987.
- [10] S. Hayati and M. Mirmirani, "Improving the absolute positioning accuracy of robot manipulators," *J. Robotic Syst.*, vol. 2, no. 4, pp. 397-413, Winter 1985.
- [11] R. N. Vaishnav and E. B. Magrab, "General procedure to evaluate robot positioning errors," *The Int. J. Robotics Res.*, vol. 6, no. 1, pp. 59-74, Spring 1987.
- [12] J. F. Figueroa, "An ultrasonic ranging system for robot end-effector position measurement," Ph.D. Dissertation, Mech. Eng. Dept., Pennsylvania State Univ., Aug. 1988.
- [13] C. C. Ruokangas *et al.*, "Integration of multiple sensors to provide flexible control strategies," *IEEE Int. Conf. Robotics Automat.*, vol. 3, pp. 1947-1953, Apr. 1986.
- [14] J. S. Showenwald and C. V. Smith, "Two-tone CW acoustic ranging technique for robot control," in *1984 IEEE Ultrason. Symp. Proc.*, pp. 469-474.
- [15] J. S. Showenwald *et al.*, "Application of acoustics to control kinematic and dynamic behavior in robots," in *1986 IEEE Ultrason. Symp. Proc.*, pp. 539-544.
- [16] C. Biber *et al.*, "The Polaroid ultrasonic ranging system," *Audio Eng. Soc.*, 67th. Convention, Tech. Paper 1696 (A-8), Oct. 31-Nov. 3, 1980, New York.
- [17] J. D. Fox, B. T. Khuri-Yakub, and G. S. Kino, "High frequency acoustic wave measurement in air," in *1983 IEEE Ultrason. Symp. Proc.*, pp. 581-584.
- [18] T. Ono, M. Kohata and T. Miyamoto, "Ultrasonic phase-sensitive rangefinder with double modulation doppler-free method for shallow seafloor survey," in *1984 IEEE Ultrason. Symp. Proc.*, pp. 480-483.
- [19] C. H. Wu and R. P. Paul, "Resolved motion force control of robot manipulator," *IEEE Trans. Syst. Man Cybern.*, vol. SMC-12, no. 3, pp. 266-275, 1982.
- [20] A. Wald, *Sequential Analysis*. New York: Wiley, 1947.
- [21] A. N. Shiryaev, *Optimal Stopping Rules*. New York: Springer-Verlag, 1978.
- [22] W. R. Hamilton, *Elements of Quaternions*. New York: Chelsea, 1969.
- [23] R. P. Paul, *Robot Manipulator: Mathematics, Programming and Control*. Cambridge, MA: MIT Press, 1981.
- [24] G. Strang, *Linear Algebra and Its Applications*. New York, Academic, 1980.
- [25] J. S. Showenwald and J. F. Martin, "PVF2 transducers for acoustic ranging and imaging in air," in *1983 IEEE Ultrason. Symp. Proc.*, pp. 577-580.
- [26] H. E. Bass and L. N. Bolen, "Ultrasonic background noise in industrial environments," *J. Acoust. Soc. Am.*, vol. 78, no. 6, pp. 2013-2016, Dec. 1985.